

LEAP: Scaling Numerical Optimization Based Synthesis Using an Incremental Approach

Ethan Smith^a, Marc G. Davis^a, Jeffrey M. Larson^b, Ed Younis^c, Costin Iancu^c, and Wim Lavrijsen^c

^aUniversity of California, Berkeley, ethanhs@berkeley.edu, marc.davis@berkeley.edu

^bArgonne National Laboratory, jmlarson@anl.gov

^cLawrence Berkeley National Laboratory, edyounis@lbl.gov, cciancu@lbl.gov, wlavrijsen@lbl.gov

Abstract

While showing great promise, circuit synthesis techniques that combine numerical optimization with search over circuit structures face scalability challenges due to large number of parameters, exponential search spaces, and complex objective functions. The LEAP algorithm improves scaling across these dimensions using iterative circuit synthesis, incremental reoptimization, dimensionality reduction, and improved numerical optimization. LEAP draws on the design of the optimal synthesis algorithm QSearch by extending it with an incremental approach to determine constant prefix solutions for a circuit. By narrowing the search space, LEAP improves scalability from four to six qubit circuits. LEAP was evaluated with known quantum circuits such as QFT and physical simulation circuits like the VQE, TFIM and QITE. LEAP is able to compile four qubit unitaries up to $59\times$ faster than QSearch and five and six qubit unitaries with up to $1.2\times$ fewer CNOTs compared to the advanced QFAST package. LEAP is able to reduce the CNOT count by up to $48\times$, or $11\times$ on average, compared to the IBM Qiskit compiler. Although employing heuristics, LEAP has generated optimal depth circuits for all test cases where a solution is known a priori. The techniques introduced by LEAP are applicable to other numerical optimization based synthesis approaches.

1 Introduction

Quantum synthesis techniques generate circuits from high-level mathematical descriptions of an algorithm. They can provide a powerful tool for circuit optimization, hardware design exploration, and algorithm discovery. An important quality metric of synthesis and compilers in general is circuit depth, which relates directly to the program performance on hardware. Short-depth circuits are especially important for noisy intermediate-scale quantum (NISQ) era devices, characterized by limited coherence time and noisy gates; here synthesis provides a critical capability in enabling experimentation.

In general, two concepts are important when thinking about synthesis algorithms [1–6]: circuit *structure* captures the application of gates on a “physical” qubit/link, while *function* captures the gate operations, for example, rotation angle $R_z(\theta)$. Recently introduced techniques [6, 7] are able to generate short-depth circuits in a topology-aware manner by combining numerical optimization of parameterized gate representations (e.g., U_3) to determine function together with search over circuit structures. Regarding circuit depth, their efficacy surpasses that of traditional optimizing compilers such as IBM Qiskit [8] or other available synthesis tools such as UniversalQ¹ [9].

Exemplary of synthesis approaches is QSearch [6], which provides optimal-depth synthesis and has been shown to match known optimal quantum algorithm implementations for circuits such as QFT [10]. QSearch

¹The UniversalQ algorithms have been recently incorporated into IBM Qiskit. For brevity, in the rest of this paper we will refer to it as Qiskit-synth.

grows a circuit by adding layers of parameterized gates and permuting gate placement at each link, building on the previous best placements to form a circuit *structure*. A numerical optimizer is run on each candidate circuit structure to instantiate the *function* that “minimizes” a score (distance from the target based on the Hilbert–Schmidt norm). This score guides the A* search algorithm [11] to extend and evaluate the next partial solution.

The QSearch behavior is canonical for numerical-optimization-based synthesis [3, 4, 6, 7]. While providing good-quality results, however, these techniques face scalability challenges: (1) the number of parameters to optimize grows with circuit depth; (2) the number of intermediate solutions to consider is exponential; and (3) the objective function for optimization is complex, and optimizers may get stuck in local minima. LEAP (Larger Exploration by Approximate Prefixes) has been designed to improve the scalability of QSearch, and it introduces several novel techniques directly extensible to the broader class of search or numerical-optimization-based synthesis.

Prefix Circuit Synthesis: Designed to improve scaling, LEAP prunes the search space by limiting backtracking depth and by coarsening the granularity of the backtrack steps. Our branch-and-bound algorithm monitors progress during search, and employs “execution-driven” heuristics to decide which partial solutions are good prefix candidates for the final solution. Whenever a prefix is chosen, the question is whether to reuse the structure (gate placement) or structure and function (gate instantiation) together. The former approach prunes the search space, while the latter prunes both the search and parameter spaces.

Incremental Reoptimization: The end result of incremental prefix synthesis (or other divide-and-conquer methods, partitioning techniques, etc.) is that circuit pieces are processed in disjunction, with the potential of missing the global optimum. Intuitively, LEAP gravitates toward the solution by combining local optimization on disjoint sub-circuits. By chopping and combining pieces of the final circuit, we can create new, unseen sub-circuits for the optimization process. Overall, this technique is designed to improve the solution quality for any divide-and-conquer or other hierarchical approach.

Dimensionality Reduction: This technique could improve both the quality of solution and the scalability. QSearch and LEAP require sets of gates that can fully describe the Hilbert subspace explored by the input transformation. This approach ensures convergence, but in many cases it may overfit the problem. We provide an algorithm to delete any parameterized gates that do not contribute to the solution, thereby reducing the dimension of the optimization problems. When applied directly to the final solution, dimensionality reduction may improve the solution quality by deleting single-qubit gates. Dimensionality reduction may also be applied in conjunction with prefix circuit synthesis, improving both scalability and solution quality.

Multistart Numerical Optimization: This technique affects both scalability and the quality of the solution. Any standalone numerical optimizer is likely to have a low success rate when applied to problem formulations that involve quantum circuit parameterizations. Multistart [12] improves on the success rate and quality of solution (avoids local minima) by running multiple numerical optimizations in conjunction. Each individual multi-optimization step may become slower, but improved solutions may reduce the chance of missing an optimal solution.

LEAP has been implemented as an extension to QSearch, and it has been evaluated on traditional “gates” such as `mul` and `adder`, as well as full-fledged algorithms such as QFT [10], HLF [13], VQE [14], TFIM [15, 16], and QITE [17]. We compare its behavior with state-of-the-art synthesis approaches: QSearch, QFAST [7], and Qiskit-synth [9]. While QSearch scales up to four qubits, LEAP is able to compile four-qubit unitaries up to 59× faster than QSearch and scales up to six qubits. On well-known quantum circuits such as the Variational Quantum Eigensolver (VQE), the quantum Fourier transform (QFT), and physical simulation circuits such as the transverse field Ising model (TFIM), LEAP with reoptimization is able to reduce the CNOT count by up to 48×, or 11× on average. Our heuristics do not affect solution quality, and LEAP can match optimal-depth solutions where available. At five and six qubits, LEAP synthesizes circuits with up to 1.19× fewer CNOTs on average compared with QFAST, albeit with an average 3.55× performance penalty. LEAP can be one order of magnitude slower than Qiskit-synth, while providing two or more orders of magnitude shorter circuits.

All of our techniques affect behavior and performance in a nontrivial way:

- Compared with QSearch, prefix synthesis reduces by orders of magnitude the number of partial solu-

tions explored, leading to significant speedup.

- Incremental reoptimization reduces circuit depth by 15% on average, without significantly affecting running time.
- Dimensionality reduction eliminates up to 40% of U_3 gates (parameters) and shortens the circuit critical path.
- Multistart increases the optimizer success rate from 15% (best value observed for any standalone optimizer) to 99%. For a single optimization run, however, multistart is up to $10\times$ slower than the underlying numerical optimizer.

Overall, we believe LEAP provides the best-quality circuit optimizer available today for circuits up to six qubits. We believe that our techniques can be easily generalized or transferred directly to other algorithms based on search of circuit structures or numerical optimization. For example, reoptimization, dimensionality reduction, and multistart are directly applicable to QFAST; and reoptimization is applicable to Qiskit-synth. We can expect that synthesis techniques using divide-and-conquer or partitioning methods will be mandatory for scalability to the number of qubits (in thousands) provided by future near-term processors. Our techniques provide valuable information to these budding approaches.

The rest of this paper is structured as follows. In Section 2 we describe the problem and its challenges. The proposed solutions are discussed in Sections 3 through 6. The experimental evaluation is presented in Section 7. In Section 9 we discuss the implications of our approach. Related work is presented in Section 10. In Section 11 we briefly summarize our conclusions.

2 Background

In quantum computing, a qubit is the basic unit of quantum information. The general quantum state is represented by a linear combination of two orthonormal basis states (basis vectors). The most common basis is the equivalent of the 0 and 1 values used for bits in classical information theory, respectively $|0\rangle = \begin{pmatrix} 1 \\ 0 \end{pmatrix}$ and $|1\rangle = \begin{pmatrix} 0 \\ 1 \end{pmatrix}$.

The generic qubit state is a superposition of the basis states, namely, $|\psi\rangle = \alpha|0\rangle + \beta|1\rangle$, with complex amplitudes α and β , such that $|\alpha|^2 + |\beta|^2 = 1$.

The prevalent model of quantum computation is the circuit model introduced in [18], where information carried by qubits (wires) is modified by quantum gates, which mathematically correspond to unitary operations. A complex square matrix U is **unitary** if its conjugate transpose U^* is its inverse, that is, $UU^* = U^*U = I$.

In the circuit model, a single-qubit gate is represented by a 2×2 unitary matrix U . The effect of the gate on the qubit state is obtained by multiplying the U matrix with the vector representing the quantum state $|\psi'\rangle = U|\psi\rangle$. The most general form of the unitary for a single-qubit gate is the “continuous” or “variational” gate representation.

$$U_3(\theta, \phi, \lambda) = \begin{pmatrix} \cos\frac{\theta}{2} & -e^{i\lambda}\sin\frac{\theta}{2} \\ e^{i\phi}\sin\frac{\theta}{2} & e^{i\lambda+i\phi}\cos\frac{\theta}{2} \end{pmatrix}$$

A quantum transformation (algorithm, circuit) on n qubits is represented by a unitary matrix U of size $2^n \times 2^n$. A circuit is described by an evolution in space (application on qubits) and time of gates. Figure 1 shows an example circuit that applies single-qubit and CNOT gates on three qubits.

Circuit Synthesis: The goal of circuit synthesis is to decompose unitaries from $SU(n)$ into a product of terms, where each individual term (e.g., from $SU(2)$ and $SU(4)$) captures the application of a quantum gate on individual qubits. This is depicted in Figure 1. The quality of a synthesis algorithm is evaluated by the number of gates in the resulting circuit and by the solution distinguishability from the original unitary.

Circuit length provides one of the main optimality criteria for synthesis algorithms: shorter circuits are better. CNOT count is a direct indicator of overall circuit length, since the number of single-qubit generic gates introduced in the circuit is proportional to a constant given by decomposition (e.g., $ZXZXZ$) rules. Since CNOT gates have low fidelity on NISQ devices, state-of-the-art approaches [1, 2] directly attempt to minimize their count. Longer-term, single-qubit gate count (and circuit critical path) is likely to augment the quality metric for synthesis.

Synthesis algorithms use distance metrics to assess the solution quality. Their goal is to minimize $\|U - U_S\|$, where U is the unitary that describes the transformation and U_S is the computed solution. They choose an error threshold ϵ and use it for convergence, $\|U - U_S\| \leq \epsilon$. Early synthesis algorithms used the diamond norm, while more recent efforts [4, 19] use the Hilbert–Schmidt inner product between the conjugate transpose of U and U_S .

$$\langle U, U_S \rangle_{HS} = \text{Tr}(U^\dagger U_S) \quad (1)$$

This is motivated by its lower computational overhead.

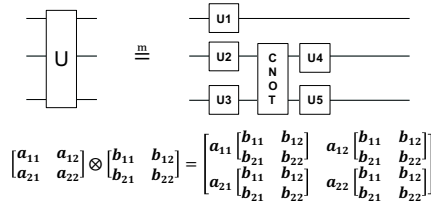


Figure 1: *Unitaries (above) and tensor products (below). The unitary U represents a $n = 3$ qubit transformation, where U is a $2^n \times 2^n$ (8×8) matrix. The unitary is implemented (equivalent or approximated) by the circuit on the right-hand side. The single-qubit unitaries are 2×2 matrices, while CNOT is a $2^2 \times 2^2$ matrix. The computation performed by the circuit is $(I_2 \otimes U_4 \otimes U_5)(I_2 \otimes \text{CNOT})(U_1 \otimes U_2 \otimes U_3)$, where I_2 is the identity 2×2 matrix and \otimes is the tensor product operator. The right-hand side shows the tensor product of 2×2 matrices.*

2.1 Optimal-Depth Topology-Aware Synthesis

QSearch [6] introduces an optimal-depth topology-aware synthesis algorithm that has been demonstrated to be extensible across native gate sets (e.g., $\{R_X, R_Z, \text{CNOT}\}$, $\{R_X, R_Z, \text{SWAP}\}$) and to multilevel systems such as qutrits.

The approach employed in QSearch is canonical for the operation of other synthesis approaches that employ numerical optimization. Conceptually, the problem can be thought of as a search over a tree of possible circuit structures containing parameterized gates. A search algorithm provides a principled way to walk the tree and evaluate candidate solutions. For each candidate, a numerical optimizer instantiates the function (parameters) of each gate in order to minimize some distance objective function.

QSearch works by extending the circuit structure a layer at a time. At each step the algorithm places a two-qubit expansion operator in all legal placements. The operator contains one CNOT gate and two $U_3(\theta, \phi, \lambda)$ gates. QSearch then evaluates these candidates using numerical optimization to instantiate *all* the single-qubit gates in the structure. An A* [11] heuristic determines which of the candidates is selected for another layer expansion, as well as the destination of the backtracking steps. Figure 2 illustrates this process for a three-qubit circuit.

Although theoretically able to solve for any “program” (unitary) size, the scalability of QSearch is limited in practice to four-qubit programs because of several factors. The A* strategy determines the number of solutions evaluated: at best this is linear in depth; at worst it is exponential. Any technique to reduce the number of candidates, especially when deep, is likely to improve performance. Our prefix synthesis solution is discussed further in Section 3.

Since each expansion operator has two U_3 gates, accounting for six² parameters, circuit parameterization

²In practice, QSearch uses 5 parameters because of commutativity rules between single-qubit and CNOT gates.

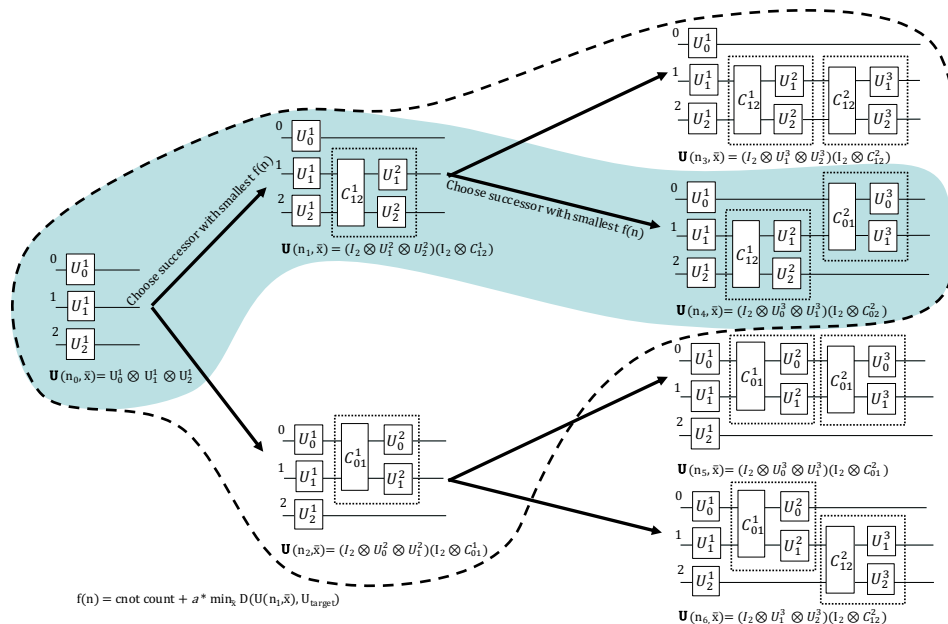


Figure 2: *Example evolution of the search algorithm for a three-qubit circuit. We start by placing a layer of single-qubit gates, then generate the next two possible solutions. Each is evaluated, and in this case the upper circuit is closer to the target unitary, leading to a smaller heuristic value. This circuit is then expanded with its possible two successors. These are again instantiated by the optimizer. The second circuit from the top has an acceptable distance and is reported as the solution. The path in blue shows the evolution of the solution. The ansatz circuits enclosed by the dotted line have been evaluated during the search.*

grows linearly with depth. Numerical optimizers scale at best with a high-degree polynomial in the number of parameters, making optimization of long circuits challenging. Any technique to reduce the number of parameters is likely to improve performance. Dimensionality reduction is discussed further in Section 5.

The scalability and the quality of the numerical optimizer matter. Faster optimizers are desirable, but their quality affects performance nontrivially. Our experimentation with CMA-ES [20], L-BFGS [21], and Google Ceres [22] shows that the QSearch success rate of obtaining a solution can vary from 20% to 1% for longer circuits. Besides this measurable outcome, the propensity of optimizers to get stuck in local minima and plateaus can have an insidious effect on scalability by altering the search path. A more nuanced approach to optimization and judicious allocation of optimization time budget may improve scalability. Our multistart approach is discussed further in Section 6.

3 Prefix Circuit Synthesis

The synthesis solution space can be thought of as a tree that enumerates circuit structures of increasing depth: Level 1 contains depth-one structures, Level 2 contains depth-two circuits, and so on. For scalability we want to reach a solution while evaluating the least number of candidates possible *and* the shallowest circuits possible. The number of evaluations is given by the search algorithm: in the case of QSearch the path is data driven by A^* , and scalability is definitely limited by long backtracking chains.

Our idea introduces a simple heuristic to reduce the frequency of backtracking. The approach is “data driven” and inspired by techniques employed in numerical optimization, as shown in Figure 3. Imagine mapping the search tree onto an optimization surface, which will contain plateaus and local minima. Exiting a plateau is characterized by faster progress toward a solution and minima. If the minima are local (partial solution is not acceptable), the algorithm has to walk out of the “valley.” Once out, the algorithm may still be on a plateau, but it can mark the region just explored as not “interesting” for any backtracking. The

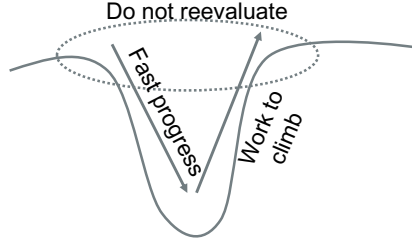


Figure 3: *Synthesis needs to navigate around local minima and plateaus.*

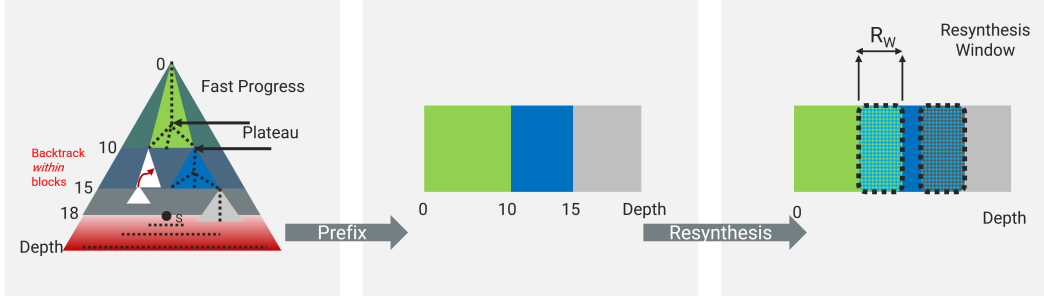


Figure 4: *Prefix-based synthesis induces a partitioning of the circuit. Each partition/prefix captures the effect of its associated subtree on the search for solution. Each partition has been subject to optimization: global with respect to the partition itself, but local with respect to the final solution. The resulting circuit in the middle reaches a solution from composing local optima. Reoptimization combines disjoint partitions in order to form regions that are passed through optimization. Since the new regions have not been subject to optimization, there exists the potential for improvement.*

effect of implementing these principles in the search is illustrated in Figure 4. The result is a partitioning of the solution space into coarse-grained regions grouped by circuit depth range. During search, backtracking between solutions within a region is performed by using the A* rules. We never backtrack outside of a region to any candidate solution that resides in the previous “depth band.”

Overall, the effect of our strategy can be thought of as determining a prefix structure on the resulting circuit, as shown in Figure 4. The algorithm starts with pure A* search on circuits of depth $[0..d_1]$ for some initial depth d_1 . The first depth d_1 viable partial solution is recorded, and the search proceeds to depth 11 in subtree A. A* search proceeds in subtree A until finding the first viable candidate at depth d_2 , then proceeds in subtree B. At this point we have three regions: the start subtree for $[0..d_1]$, A for $[d_1 + 1..d_2]$, and B for $[d_2 + 1..d_3]$ depth. In this example the search in subtree B fails at depth $d_2 + 1$. We therefore backtrack to d_2 , and the search proceeds on the path depicted on the right-hand side of the tree and eventually finds a solution.

One can easily see how by prohibiting backtracking into large solution subtrees we can reduce the number of evaluated (numerically optimized) candidates and improve scalability. As this changes the A* optimality property of the algorithm, the challenge is determining these subtrees in a manner that still leads to a short-depth solution.

Prefix Formation: A partial solution describes a circuit structure and its function (gates). We have considered both static and dynamic methods for prefix formation. In our nomenclature, a static approach will choose a prefix circuit whose structure and function are fixed: this is a fully instantiated circuit. A dynamic approach will choose a fixed structure whose function is still parameterized. In the first case, the prefix circuit is completely instantiated with native gates to perform a single computation, while in the latter it can “walk” a much larger Hilbert subspace as induced by the parameterization. Intuitively, determining a single instantiated prefix circuit is good for scalability. This reduces the number of parameters evaluated in any numerical optimization operation subsequent to prefix formation. We have experimented with several

strategies for forming instantiated prefix circuits in our synthesis algorithms, but they did not converge or produced very long circuits.

Prefix Formulation: In LEAP we use a dynamic data-driven approach informed by the evolution of the underlying A* QSearch algorithm, described in Figure 4. Our analysis of the trajectories for multiple examples shows that many paths are characterized by a rapid improvement in solution quality (reduction in Hilbert–Schmidt distance between target unitary and approximate prefix), followed by plateauing induced either by optimizer limitations (local minima) or as an artifact of the particular structures considered (dead-end).

LEAP forms subtrees by first identifying and monitoring plateaus. Since during a plateau the rate of solution quality change is “low,” a “prefix” is formed whenever a solution is evaluated with a jump in the rate of change. The plateau identification heuristic is augmented with a work-based heuristic: we wait to form a prefix until we sample enough partial solutions on a path. This serves several purposes: it gives us more samples in a subtree to gain some confidence we have not skipped “the only few viable partial solutions,” and it increases the backtracking granularity by identifying larger subtrees. Even more subtly, the work heuristic decreases the sensitivity of the approach to the thresholds used to assess the rate of change in the plateau identification method. By delaying to form a prefix based on work, we avoid jumping directly into another plateau that will result in superfluously evaluating many solutions close in depth to each other.

Solution Optimality: By discarding the A* search, LEAP gives up on always finding the optimal solution. However, the following observations based on the properties of the solution search space indicate that optimality loss could be small and that the approach can be generalized to other search and numerical optimization-based methods.

First, the solution tree of circuit structures exhibits high symmetry. Partial solutions can be made equivalent by qubit relabeling; all solutions reached from any equivalent structure will have a similar depth. For example, for a circuit with N qubits, a depth 1 circuit with a CNOT on qubits 0 and 1 can be thought as “equivalent” to the circuit with a CNOT on qubits $N - 2$ and $N - 1$. Symmetry indicates that coarse-grained pruning may be feasible, since a subtree may contain many “equivalent” partial solutions.

Second, assuming that the optimal solution has depth d , there are many easy-to-find solutions at $depth > d$. In Figure 3, assume that the solution node S at depth d is missed by our strategy. However, there are $links$ solutions at $d + 1$, $links^2$ solutions at $d + 2$, and so forth, trivially obtained by adding identity gates to S . In other words, the solution density increases (probably quadratically) with circuit depth increase. If the search has a “decent” partial solution at depth d , numerical optimization is likely to find the final solution at very close depth. Overall, the high-level heuristic goal is to get to optimal depth with a “good enough” partial solution. Our “good enough” criteria combine the Hilbert–Schmidt norm with a measure of work.

The pseudocode for the prefix formation algorithm in LEAP is presented in Figure 5.

4 Incremental Reoptimization

The end result of incremental synthesis (or other divide-and-conquer methods, partitioning techniques, etc.) is that circuit pieces are optimized in disjunction, with the potential of missing the optimal solution. For LEAP, this is illustrated in Figure 4. Prefix synthesis generates a natural partitioning of the circuit. Each partition is optimized based on knowledge local to its subtree. The final solution is composed of local optima. The basic observation here is that by chopping and combining pieces of the circuit generated by prefix synthesis, we can create new, unseen circuits for the optimization process.

For incremental reoptimization we use the output circuit from prefix synthesis and its partitioning (the list of depths where prefixes were fixed). The reoptimizer removes circuit segments to create “holes” of a size provided by the user (referred to as reoptimization window) centered on the divisions between partitions. This circuit is lifted to a unitary, and the reoptimizer synthesizes it and replaces it into the original solution. The process continues iteratively until a stopping criterion is reached. This amounts to moving a sliding optimization window across the circuit.

The quality of the solution is determined by the choice of the size of the reoptimization window, the number of applications (circuit coverage) and stopping criteria, and the numerical optimizer.

Algorithm 1 Helper Functions

```
1: function  $s(n)$ 
2:   return  $\{n + \text{CNOT} + U_3 \otimes U_3 \text{ for all possible CNOT positions}\}$ 
3:
4: function  $P(n, U)$ 
5:   return  $\min_{\bar{x}} D(U(n, \bar{x}), U)$ 
6:
7: function  $H(d)$ 
8:   return  $d * a$   $\triangleright a$  is a constant determined via
   experiment. See section 3.3.1
9:
10: function  $\text{PREDICT\_SCORE}(a, b, d_i)$ 
11:   return  $\{\text{Predicted CNOTs for depth } d_i \text{ based on points in } a, b\}$ 
```

Algorithm 2 LEAP Prefix Formation

```
1: function  $\text{LEAP\_SYNTHESIZE}(U_{\text{target}}, \epsilon, \delta)$ 
2:    $s_i \leftarrow$  the best score of prefixes
3:    $n_i \leftarrow$  the prefix structure
4:   while  $s_i > \epsilon$  do
5:      $n_i, s_i \leftarrow \text{INNER\_SYNTHESIZE}(U_{\text{target}}, \epsilon, \delta)$ 
6:   return  $n_i, s_i$ 
7:
8: function  $\text{INNER\_SYNTHESIZE}(U_{\text{target}}, \epsilon, \delta)$ 
9:    $n \leftarrow$  representation of  $U_3$  on each qubit
10:   $a \leftarrow$  best depth values of intermediate results
11:   $b \leftarrow$  best depth values of intermediate results
12:  push  $n$  onto queue with priority  $H(d_{\text{best}})+0$ 
13:  while queue is not empty do
14:     $n \leftarrow$  pop from queue
15:    for all  $n_i \in S(n)$  do
16:       $s_i \leftarrow P(n_i, U_{\text{target}})$ 
17:       $d_i \leftarrow$  CNOT count of  $n_i$ 
18:       $s_p \leftarrow \text{PREDICT\_SCORE}(a, b, d_i)$ 
19:      if  $s_i < \epsilon$  then
20:        return  $n_i, s_i$ 
21:      if  $s_i < s_p$  then
22:        return  $n_i, s_i$ 
23:      if  $d_i < \delta$  then
24:        push  $n_i$  onto queue with priority
 $H(d_i)+\text{CNOT count of } n_i$ 
```

Figure 5: Prefix formation algorithm in LEAP, based on the algorithm in [6].

In LEAP we make several pragmatic choices. The size of the optimization window is selected to be long enough for reduction potential but overall short enough that it can be optimized fast enough. The algorithm reoptimizes exactly once at each boundary in the original partitioning. The reoptimization pass allows us to manage the budget given to numerical optimizers. Since each circuit piece is likely to be transformed multiple times, some of the operations can use fast but lower-quality/budget optimization. We do use the fastest optimizer available during prefix synthesis, switching during reoptimization to the higher-quality but slower multistart solver based on [12], described in Section 6.

5 Dimensionality Reduction

The circuit solution provides a parameterized structure instantiated for the solution. This parameterization introduced by the single-qubit U_3 gates may overfit the problem.

For LEAP, which targets only the CNOT count, this may be a valid concern, and we therefore designed a dimensionality reduction pass. We use a simple algorithm that attempts to delete one U_3 gate at a time and reinstantiates the circuit at each step. This linear complexity algorithm can discover and remove only simple correlations between parameters. More complex cases can be discovered borrowing from techniques for dimensionality reduction for machine learning [23] or numerical optimization [24].

When applied on the final synthesis solution, dimensionality reduction may reduce the circuit critical path even further by deleting U_3 gates. It can also be combined with the prefix synthesis. Once a prefix is formed, we can reduce its dimensionality. As numerical optimizers scale exponentially with parameters, this will improve the execution time per invocation. On the other hand, it may affect the quality of the solution as we remove expressive power from prefixes. In the current LEAP version, only the final solution is simplified.

6 Multistart Optimization

Solving the optimization problem for the objective function in LEAP or QSearch can be difficult. Quantum circuits, even optimal ones, are not unique: a global phase is physically irrelevant and thus does not affect the output. Furthermore, circuits that differ only in a local basis transformation and its inverse surrounding a circuit subsection (e.g., a single 2-qubit gate) are mathematically equivalent.³ Provided native gate sets may contain equivalences; and single-qubit gates, being rotations, are periodic. As a practical matter, we find that we cannot declare these equivalences to existing optimizers; and where they can be used to create constraints or inaccessible regions (e.g., by remapping the periodicity into a single region), we find that they hinder the search more than help, because boundaries can create artificial local minima.

The unavoidable presence of equivalent circuits means that we are essentially overfitting the problem, where changes in parameters can cancel each other out, leading to saddle points, which turn into local minima in the optimization surface because of the periodicity; see Figure 6. The former cause, at best, an increase in the number of iterations as progress slows down because of smaller gradients; the latter risks the optimizer getting stuck.

Another problem comes from the specification of the objective: distance metrics care only about the output, and different circuits can thus result in equal distances from the desired unitary. If no derivatives are available, this results in costly evaluations just to determine no progress can be made, a problem that gets worse at scale. But even with a derivative, it closes directions for exploration and shrinks viable step sizes, thus increasing the likelihood of getting stuck in a local minimum.

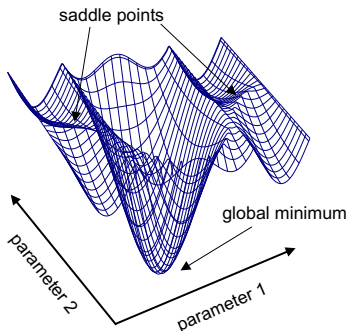


Figure 6: Optimization surface near the global minimum for a 4-qubit circuit of depth 6 for the first step in the QITE algorithm, varying 6 (3 pairs) out 42 parameters equally, showing the effect on the optimization surface for 2 parameters from distinct pairs. (The global minimum is so pronounced only because the remaining 36 parameters are kept fixed at optimum, reducing the total search space; most of the 42-dim surface is actually flat.

In sum, local optimization methods are highly dependent on the starting parameters, yet global optimization methods can require far too many evaluations to be feasible for real-world objectives. An attractive middle ground can be approached that start local optimization runs from different points in the domain. Multistart optimization methods are especially appealing when there is structure in the objective, such as the least squares form of the objective.

Some multistart approaches complete a given local optimization run before starting another, whereas others may interleave points from different runs. The asynchronously parallel optimization solver for finding multiple minima (APOSMM) [12] begins with a uniform sampling of the domain and then starts local optimization runs from any point subject to constraints: (1) point not yet explored; (2) not a local optimum; and (3) no point available within a distance r_k with a smaller function value. If no such point is available, more sampling is performed. The radius r_k decreases as more points are sampled, thereby allowing past points to start runs. Under certain conditions on the objective function and the local optimization method,

³There are physical differences; in particular such circuits tend to sample different noise profiles. This property forms the basis of randomized compilation.

	All-to-all				Linear			
	Mapped	LEAP	QFAST	Qiskit	Mapped	LEAP	QFAST	Qiskit
Time (s)	<1	7.34e3	423	31	1.4	608	342	76
Error	1e-16	1e-12	1e-4	1e-11	2.9e-1	1e-12	1e-5	9e-1
CNOT	240	18.85	27.8	1991	250	18.8	36.4	6115
U_3	270	41.71	60.9	2155	291	42.7	78.2	9512
Depth	207	29.2	43.9	3912	321	28	48.6	9004

Table 1: Summary of the quality metrics (average value) for five- and six-qubit circuit synthesis.

the logic of APOSMM can be shown to asymptotically identify all local optima while starting only finitely many local optimization runs.

7 Experimental Setup

LEAP, available at <https://github.com/BQSKit/qsearch>, extends QSearch. We evaluated it with Python 3.8.5, using numpy 1.19.5 and Rust 1.48.0 code.

For our APOSMM implementation, we integrated the implementation in the libEnsemble Python package [25, 26]. We tried two different local optimization methods within APOSMM: the L-BFGS implementation within SciPy [21] and the Google Ceres [22] least-squares local optimization routine.

For experimental evaluation we use a 3.35GHz Epyc 7702p based server, with 64 cores and 128 threads. Our workload consists of known circuits (e.g., mul, add, quantum Fourier transform), as well as newly introduced algorithms. VQE [14] starts with a parameterized circuit and implements a hybrid algorithm where parameters are reinstantiated based on the results of the previous run. The TFIM [15] and quantum imaginary time evolution (QITE) [17] algorithms model the time evolution of a system. They are particularly challenging for NISQ devices as circuit length grows linearly with the simulated time step. In TFIM, each timestep (extension) can be computed and compiled ahead of time from first principles, while in QITE it is dependent on the previous time step.

We evaluate LEAP against QSearch and other available state-of-the-art synthesis software and compilers. QFAST [27] provides better scalability than does QSearch by conflating search for structure with numerical optimization, albeit producing longer circuits. Qiskit-synth [9] uses linear algebra decomposition rules for fast synthesis, but circuits tend to be long. IBM Qiskit [8] provides “traditional” quantum compilation infrastructures using peephole optimization and mapping algorithms. To showcase the impact of QPU topology, we compile for processors where qubits are fully connected (all-to-all), as well as processors with qubits connected in a nearest-neighbor (linear) fashion.

8 Evaluation

Summarized results are presented in Figure 6, with more details in Tables 2 and 3. For most three- and four-qubit benchmarks, the reference implementations are already optimal when mapped to an all-to-all chip topology. Consequently we present data only for compilations onto a chip nearest-neighbor topology. For five- and six-qubit benchmarks we present data for all-to-all and nearest-neighbor chip topology.

Table 2 presents a direct comparison between QSearch and LEAP for circuits up to four qubits. Despite its heuristics, LEAP produces optimal depth solutions, matching the reference implementations on nearest-neighbor chip topology. Overall, LEAP is able to compile four-qubit unitaries up to $59\times$ faster than QSearch.

As shown in Table 3, LEAP scales up to six qubits. In this case we include full topology data, as well results for compilation with QFAST, Qiskit, and Qiskit-synth. On well-known quantum circuits such as VQE and QFT and on physical simulation circuits such as TFIM, LEAP with reoptimization is able to reduce the CNOT count by up to $48\times$, or $11\times$ on average. Our heuristics do not affect solution quality, and LEAP can match optimal depth solutions where available. At five and six qubits, LEAP synthesizes circuits with to $1.19\times$ fewer CNOTs on average compared with QFAST, albeit with an average $3.55\times$ performance

			QSearch			LEAP		
ALG	Qubits	Ref	CNOT	Unitary Distance	Time (s)	CNOT	Unitary Distance	Time (s)
QFT	3	6	7	$3.33 * 10^{-16}$	2.0	8	$2.22 * 10^{-16}$	1.7
Toffoli	3	6	8	$2.22 * 10^{-16}$	3.4	8	$2.22 * 10^{-16}$	1.6
Fredkin	3	8	8	$4.44 * 10^{-16}$	2.6	8	$3.33 * 10^{-16}$	1.7
Peres	3	5	7	0	1.7	7	$2.22 * 10^{-16}$	1.1
Logical OR	3	6	8	$2.22 * 10^{-16}$	3.4	8	$3.33 * 10^{-16}$	1.6
QFT	4	12	14	$6.7 * 10^{-16}$	2429.3	13	$6.7 * 10^{-16}$	77.9
TFIM-1	4	6	6	0	13.4	6	0	7.2
TFIM-10	4	60	11	$9.08 * 10^{-11}$	955.4	11	$3.95 * 10^{-11}$	47.8
TFIM-22	4	126	12	$1.22 * 10^{-15}$	2450.3	12	$7.77E - 16$	41.6
TFIM-60	4	360	12	$4.44 * 10^{-16}$	1391	12	$2.22 * 10^{-16}$	31.6
TFIM-80	4	480	12	$4.44 * 10^{-16}$	1553.1	12	$2.22 * 10^{-16}$	35
TFIM-95	4	570	12	$6.66 * 10^{-16}$	1221.4	12	$2.22 * 10^{-16}$	38.1

Table 2: Summary of synthesis results for QSearch and LEAP on the linear topology. On average, LEAP produces the same results as QSearch in less time. * HLF is the hidden linear function algorithm from [13].

		5 Qubits					6 Qubits										
		grover5	hlf	mul	qaoa	qft5	TFIM-10	TFIM-40	TFIM-60	TFIM-80	TFIM-100	TFIM-1	TFIM-10	TFIM-24	TFIM-31	TFIM-51	
CNOTs	All-to-All	Qiskit Mapped	48	13	17	20	20	80	320	480	640	800	10	100	240	310	510
		LEAP	*	9	13	*	31	18	22	21	21	22	10	*	*	*	*
		QFAST	70	13	18	39	46	20	20	24	22	26	12	29	26	24	28
Qiskit Synthesized	570	870	77	750	580	1025	1025	1025	1025	1025	4006	4474	4474	4474	4474	4474	
	Qiskit Mapped	131	23	22	55	31	80	320	480	640	800	10	100	240	310	510	
	LEAP	49	15	15	28	30	18	20	20	20	20	10	24	27	29	30	
QFAST	60	55	58	69	114	12	18	20	20	21	10	16	20	22	32	32	
	2503	2578	760	3692	2922	2791	2791	2791	2791	2791	13155	13365	13365	13365	13365	13365	
	Qiskit Synthesized	672	976	87	861	687	1140	1140	1140	1140	4294	4765	4765	4765	4765	4765	
U ₃ *	All-to-All	Qiskit Mapped	78	8	16	20	29	90	360	540	720	900	11	110	264	341	561
		LEAP	*	22	27	*	65	41	49	45	47	45	26	*	*	*	*
		QFAST	145	31	41	83	97	45	45	53	49	57	30	64	58	54	62
Qiskit Synthesized	672	976	87	861	687	1140	1140	1140	1140	1140	4294	4765	4765	4765	4765	4765	
	Qiskit Mapped	235	37	40	93	63	90	360	540	720	900	11	110	264	341	561	
	LEAP	103	35	35	61	65	41	45	45	45	45	26	54	60	64	64	
QFAST	125	115	121	143	233	29	41	45	45	47	26	38	45	50	70	70	
	4008	4046	1190	4264	4165	4400	4401	4401	4401	4400	20375	20659	20658	20656	20658		
	Qiskit Synthesized	672	976	87	861	687	1140	1140	1140	1140	4294	4765	4765	4765	4765		
Depth	All-to-All	Qiskit Mapped	85	16	26	32	26	76	286	426	566	706	16	79	177	226	366
		LEAP	*	13	22	*	47	29	35	31	31	13	33	13	*	*	
		QFAST	123	21	33	65	85	31	33	49	29	39	13	47	29	29	33
Qiskit Synthesized	1064	1662	138	1451	1089	2008	2008	2008	2008	2008	7872	8841	8841	8841	8841		
	Qiskit Mapped	200	34	40	76	44	76	286	426	566	706	16	79	177	226	366	
	LEAP	71	17	29	41	45	25	27	35	35	31	13	31	31	33	37	
QFAST	99	87	77	83	151	17	21	29	21	27	13	17	25	21	45	45	
	3799	3933	1115	4061	3924	4236	4236	4236	4236	4236	19074	19495	19495	19494	19494		
	Qiskit Synthesized	672	976	87	861	687	1140	1140	1140	1140	4294	4765	4765	4765	4765		
Time (s)	All-to-All	Qiskit Mapped	0.16	0.05	0.07	0.07	0.11	0.22	0.88	1.19	1.68	2.03	0.04	0.28	0.62	0.80	1.41
		LEAP	*	618.62	652.92	*	11418.54	7826.57	16527.44	9069.7	6628.47	1586.35	19233.36	*	*	*	*
		QFAST	3187.40	27.70	86.79	249.15	499.49	79.86	69.38	71.98	77.42	215.13	23.14	618.43	191.99	270.70	684.63
Qiskit Synthesized	11.61	14.50	2.65	14.61	14.43	14.35	15.04	14.59	14.27	16.52	82.16	62.93	64.10	63.34	64.62		
	Qiskit Mapped	1.12	0.24	0.38	0.46	0.34	0.43	1.75	2.57	3.39	4.31	0.09	0.51	1.30	1.61	2.60	
	LEAP	25293.78	165.50	856.36	3525.54	5165.28	11631.55	3585.95	2113.57	1901.41	2835.3	7651.29	145903.80	175491.42	177015.25	47681.98	
QFAST	992.38	228.55	213.94	365.15	1901.26	7.67	22.78	26.63	30.28	21.01	5.25	61.68	82.52	408.35	772.39		
	33.20	34.42	12.38	36.25	38.37	35.93	35.53	32.27	34.11	32.41	170.08	161.25	156.66	161.30	159.81		
	Qiskit Synthesized	672	976	87	861	687	1140	1140	1140	1140	4294	4765	4765	4765	4765		

Table 3: Results for 5–6 qubit synthesis benchmarks with QFAST, LEAP, and IBM Qiskit. (* implies the program timed out after 12 hours.)

penalty. LEAP can be one order of magnitude slower than Qiskit-synth, while providing two or more orders of magnitude shorter circuits.

8.1 Prefix

ALG	Qubits	CNOT \updownarrow	# of Blocks	Block End Locations
fredkin	3	8	2	5,8
toffoli	3	8	2	6,9
grover3	3	7	2	5,7
hhl	3	3	1	3,
or	3	8	2	5,8
peres	3	7	2	6,7
qft3	3	8	2	5,9
qft4	4	18	4	5,13,18,21
adder	4	15	3	8,14,19
vqe	5	20	8	3,7,11,14,18,21,25,28
TFIM-1	4	7	2	5,7
TFIM-10	4	12	3	5,10,12
TFIM-22	4	12	3	5,10,12
TFIM-60	4	12	3	5,10,12
TFIM-80	4	12	3	5,10,12
TFIM-95	4	12	3	5,10,12
mul	5	15	5	3,9,12,16,18
qaoa	5	28	7	6,10,14,19,24,29,35
qft5	5	30	10	5,8,11,15,20,25,30,35,38,40
TFIM-10	5	18	7	3,6,9,13,16,19,21
TFIM-40	5	20	7	3,7,10,13,16,19,21
TFIM-60	5	20	7	3,6,10,15,18,21,24
TFIM-80	5	20	7	3,6,11,16,20,23,24
TFIM-100	5	20	6	5,9,13,17,20,22
TFIM-1	6	10	4	4,7,10,12

Table 4: Number and location of prefix blocks for various circuits.

Most of the speed improvements are directly attributable to prefix synthesis, which reduces by orders of magnitude the number of partial solutions evaluated. For example, for QFT4, the whole search space contains $\approx 43M$ solution candidates. QSearch will explore 2,823 nodes, while LEAP will explore 410. For TFIM-22, these numbers are ($\approx 1.6M$, 54,020, 176) respectively. Detailed results are omitted for brevity.

Prefix formation is calculated based on a best-fit line formed by a linear regression of the best scores versus the depth associated with the new best-found score. This linear regression is used as an estimator of the expected score at the current depth. When the score calculated from the heuristic is better than the expected score, this means that the new best score is better than expected; in other words more progress to the solution has been made than expected. We have noticed that in QSearch, when the search algorithm needs to backtrack and search many different nodes, the progress towards the solution is lower, and the calculated score is worse than the expected score. We therefore do not form prefixes in this case, which allows LEAP to maintain the important backtracking and searching that makes QSearch optimal.

Table 4 presents the number of prefixes formed during synthesis for each circuit considered. Since prefixes have a depth between three and five qubits, this informs our choice of the reoptimization window discussed below.

8.2 Incremental Reoptimization

While significantly reducing depth (with respect to the circuit reference), prefix synthesis can be improved upon by incremental reoptimization, as shown by the comparison in Table 5. LEAP applies only a single step of reoptimization. Given the solution from prefix synthesis, LEAP selects a window at each prefix boundary, resynthesizes, and reassembles the circuit. Detailed results are omitted for brevity, but further iterations do little to improve solution.

The reoptimization window in LEAP is chosen pragmatically with a limited depth (7 CNOTs for 3 and 4 qubits, 5 CNOTs for 5 and 6 qubits in our case), to lead to reasonable expectations on execution time, while providing some optimization potential.

Incremental reoptimization reduces circuit depth by 15% on average, without significantly affecting running time.

ALG	Qubits	Before Resynthesis			After Resynthesis		
		CNOT ↓	Unitary Distance	Time (s)	CNOT ↓	Unitary Distance	Time (s)
qft3	3	9	0	1.6	8	0	3.4
logical_or	3	8	$4.44 * 10^{-16}$	1.4	8	$4.44 * 10^{-16}$	5.9
fredkin	3	8	$2.22 * 10^{-16}$	1.4	8	$2.22 * 10^{-16}$	5.7
toffoli	3	9	$2.22 * 10^{-16}$	1.7	8	0	3.4
adder	4	19	0	48.9	15	$2.22 * 10^{-16}$	76.7
qft4	4	21	$2.22 * 10^{-16}$	38.6	18	$1.11 * 10^{-16}$	190.3
TFIM-10	4	12	$8.03 * 10^{-12}$	10.3	12	$8.03 * 10^{-12}$	176.6
TFIM-80	4	12	$6.66 * 10^{-16}$	4.2	12	$6.66 * 10^{-16}$	103.8
TFIM-95	4	12	$4.44 * 10^{-16}$	6.5	12	$4.44 * 10^{-16}$	113
vqe	4	28	$2.47 * 10^{-11}$	151.2	20	$2.70 * 10^{-11}$	2062.8
qft5	5	40	$1.22 * 10^{-15}$	772.4	30	$6.66 * 10^{-16}$	4392.8
TFIM-10	5	21	$7.97 * 10^{-12}$	310.6	18	$9.19 * 10^{-12}$	11320.8
TFIM-40	5	21	$6.66 * 10^{-16}$	44	20	0	3541.8
TFIM-60	5	24	0	66.9	20	0	2046.5
TFIM-80	5	24	$2.22 * 10^{-16}$	73.5	20	$2.22 * 10^{-16}$	1827.8
TFIM-100	5	22	$4.44 * 10^{-16}$	55.4	20	$1.11 * 10^{-16}$	2779.8
mul	5	18	$4.44 * 10^{-16}$	47.0	15	$2.22 * 10^{-16}$	809.2
TFIM-1	6	12	$2.22 * 10^{-16}$	213.3	10	$1.11 * 10^{-16}$	7437.9

Table 5: Summary of the CNOT reduction and time for resynthesis on the linear topology.

8.3 Dimensionality Reduction

LEAP applies a single step of dimensionality reduction at the end of the synthesis process, the sweep starting at the circuit beginning. For brevity, we omit detailed data and note that in this final stage dimensionality reduction eliminates up to 40% of U_3 gates (parameters) and shortens the circuit critical path. These results clearly indicate that our approach overfits the problem by inserting too many U_3 gates.

Name	Number of Gates Deleted									
qft2	2	0	0	0	0	0	1	1	1	
qft3	2	0	0	1	0	0	1	1	1	
fredkin	3	2	0	1	1	2	0	0	1	
toffoli	2	2	1	2	1	2	0	1	0	
peres	2	0	1	2	0	1	0	1	1	
logical_Lor	2	1	2	0	2	1	0	1	0	
hhl	2	0	2	0						

Table 6: Spatial placement of U_3 gates deleted. Number of columns denotes circuit stages (CNOT), and we present the number of gates deleted at each position.

We examined the spatial occurrence of single-qubit gate deletion since this may guide any dynamic attempts to eliminate parameters during synthesis for scalability purposes. Figure 6 presents a summary for three-qubit circuits; trends are similar for all other benchmarks considered. The data shows that gate deletion is successful at many circuit layers, indicating that a heuristic for on-the-fly dimensionality reduction heuristic may be feasible to develop for even further scalability and quality improvements. As discussed in Section 6, dimensionality reduction will reduce the number of parameters for numerical optimization, while reducing overfitting and gate (parameter) correlation that lead to cancellations of gate effects on a qubit.

8.4 Multistart Optimization

When evaluating numerical optimizers used in synthesis, we are interested in determining how often they found the true minimum, since this has a significant impact on both solution quality and execution speed.

ALG	CNOT ↓	BFGS		Ceres		APOSMM-8		APOSMM-12		APOSMM-16		APOSMM-20		APOSMM-24	
		% Success	Time (s)												
fredkin	8	89	0.03	69	0.01	100	0.13	100	0.14	100	0.14	100	0.15	100	0.16
logical_Lor	8	16	< 0.01	55	0.01	100	0.13	100	0.14	100	0.15	100	0.16	100	0.17
peres	7	18	< 0.01	73	0.01	69	0.08	90	0.11	92	0.12	98	0.13	99	0.14
toffoli	8	43	0.01	74	0.01	100	0.13	100	0.14	100	0.14	100	0.15	100	0.17
qft3	8	9	< 0.01	26	< 0.01	80	0.10	91	0.12	95	0.13	98	0.14	100	0.16
qft4	18	1	< 0.01	15	0.02	66	0.50	83	0.68	92	0.82	94	0.99	99	1.08
qft5	30	0	< 0.01	2	0.12	8	1.19	13	2.78	15	3.81	25	7.21	36	12.10

Table 7: Accuracy and speed of various optimizers on a variety of circuits. APOSMM-N means APOSMM with N starting points.

We evaluated the commonly used local optimization methods Google’s Ceres [22] and an implementation of L-BFGS [21] as well as the multistart APOSMM [12] framework.

We ran each optimizer 100 times on several circuits to evaluate their accuracy and speed. The results are summarized in 7. The QFT results illustrate that the BFGS and Ceres optimizers perform poorly even on a smaller circuit such as a three-qubit QFT, finding solutions just 9% and 26% of the time, much lower than even APOSMM with 8 starting points. We found that APOSMM with 12 starting points performed well on all but the five-qubit QFT circuit. Since optimizing the parameters of the QFT5 circuit is a much higher-dimensional problem, even APOSMM with 24 starting points found solutions in 36% of the runs.

While APOSMM is much more accurate than BFGS and Ceres on the circuits we tested, it is also about an order of magnitude slower for larger circuits, even though the local optimization runs are done in parallel. In addition, the slowdown increases with the number of starting points. The time for QFT5 approximately doubles every 4 additional starting points for parallel runs. For our runs in Table 3 we selected 12 starting points since this number was reasonably accurate and takes a reasonable amount of time.

Therefore when using LEAP, we use Ceres because it is fast and scales well, and a missed solution will be found during reoptimization. During reoptimization, APOSMM is used, since it is much more likely to find true minima, thus strengthening the optimality of search-based algorithms.

9 Discussion

Overall, the results indicate that the heuristics employed in LEAP are much faster than QSearch and are still able to produce optimal depth solutions in a topology-aware manner. The average depth difference for three- and four-qubit benchmarks between QSearch and LEAP is 0 across physical chip topologies and workload.

We find the prefix formation idea intuitive, easily generalizable, and powerful. The method used to derive prefix formation employs concepts encountered in numerical optimization algorithms and is easily identifiable in other search-based synthesis algorithms: “progress” to solution, and “region of similarity” or plateau.

The LEAP algorithm indicates that incremental and iterative approaches to synthesis work well. In our case, the results even indicate that one extra step of local optimization is able to match the efficacy of global optimization. This result bodes well for approaches that scale synthesis through circuit partitioning, such as our QGo [28] algorithm.

Dimensionality reduction as implemented in LEAP not only reduces the effects of overfitting by numerical optimization but also opens a promising path for scaling numerical-optimization-based synthesis. Since we were able to delete 40% of parameters from the final solution, we believe that by combining it with prefix synthesis we can further improve LEAP’s scalability.

Multistart optimization can be trivially incorporated into any algorithm, and we have indeed already modified the QSearch and QFAST algorithms to incorporate it. Furthermore, the spirit of the multistart “approach” can be employed to further prune the synthesis search space. Whenever a prefix formed, the synthesis algorithm had explored a plateau and a local minimum. At this stage, a multistart search could be started using as seeds other promising partial solutions within the tree.

The prefix formation idea is powerful and showcases how synthesis can turn into a capable tool. TFIM circuits simulate a time-dependent Hamiltonian, where the circuit for each time step “contains” the circuit (computation) associated with the previous time step as prefix. The circuits generated by the TFIM domain generator grow linearly in size. In our experiments, we observed that after some initial time steps, all circuits for any late time step have an asymptotic depth. This observation led to the following experiment: we picked a circuit generated for a late simulation step and considered it as a parameterized template for all other simulation steps. We then successfully solved the synthesis problem with this template for any TFIM step. This procedure empirically provides us with a fixed-depth (short-depth) template for the TFIM algorithm. Furthermore, this demonstration motivated a successful effort [29] to derive from first principles a fixed-depth circuit for TFIM. The results are presented in Figure 7. Note the highly increased fidelity when running the circuit on the IBM Athens system.

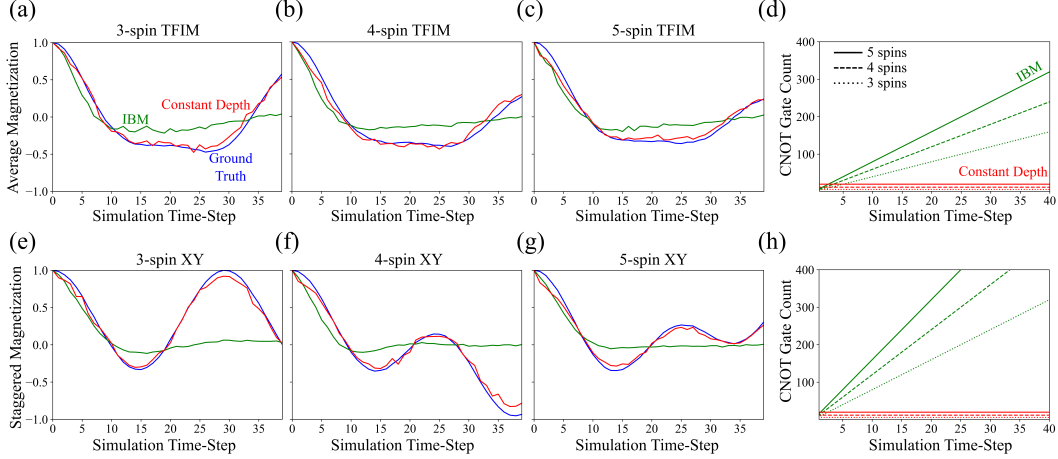


Figure 7: *TFIM circuit depth evolution and “fidelity” when executed on the IBM Athens system.*

The QITE algorithm presents an interesting challenge to the prefix formation idea. In this case, the next timestep circuit is obtained by extending the “current” circuit with a block dependent on its output after execution. When executing on hardware, synthesis has real-time constraints, and it has to deal with the hardware noise that affects the output. Preliminary results, courtesy of our collaborators Jean-Loup Ville and Alexis Morvan, indicate that the approach taken for TFIM may be successful for QITE. Table 8 summarizes the preliminary observations and indicates that again synthesis produces better-quality circuits than the domain generator or traditional compilation does. Note that in this experiment LEAP was fast enough to produce real-time results during the hardware experiment only for three-qubit circuits.

QITE size	CNOT		
	Qiskit Isometry	QFAST	LEAP
2	3	3	3
3	30-35	10-12	7-12
4	160-200	70-80	30-50

Table 8: *Summary of QITE results when running synthesis on hardware experiments. Structure of any circuit is determined by the output of the previous circuit, hence hardware noise.*

10 Related Work

A fundamental result that spurred the apparition of quantum circuit synthesis is provided by the Solovay–Kitaev (SK) theorem. The theorem relates circuit depth to the quality of the approximation, and its proof is by construction [30–32]. Different approaches [30, 33–42] to synthesis have been introduced since, with the goal of generating shorter-depth circuits. These can be coarsely classified based on several criteria: target gate set, algorithmic approach, and solution distinguishability.

Target Gate Set: The SK algorithm is applicable to any universal gate set. Later examples include synthesis of z-rotation unitaries with Clifford+V approximation [43] or Clifford+T gates [44]. When ancillary qubits are allowed, one can synthesize single-qubit unitaries with the Clifford+T gate set [44–46]. While these efforts propelled the field of synthesis, they are not used on NISQ devices, which offer a different gate set ($R_x, R_z, CNOT$ and Mølmer–Sørensen all-to-all). Several [1–3] other algorithms, discussed below, have since emerged.

Algorithmic Approaches: The early attempts inspired by the Solovay–Kitaev algorithm use a recursive (or divide-and-conquer) formulation, sometimes supplemented with search heuristics at the bottom. More

recent search-based approaches are illustrated by the meet-in-the-middle [35] algorithm.

Several approaches use techniques from linear algebra for unitary and tensor decomposition. Bullock and Markov [38] use QR matrix factorization via a Givens rotation and Householder transformation [39], but open questions remain as to the suitability for hardware implementation because these algorithms are expressed in terms of row and column updates of a matrix rather than in terms of qubits.

The state-of-the-art upper bounds on circuit depth are provided by techniques [1, 2] that use cosine-sine decomposition. The cosine-sine decomposition was first used in [47] for compilation purposes. In practice, commercial compilers ubiquitously deploy only KAK [5] decompositions for 2-qubit unitaries.

The basic formulation of these techniques is topology independent. Specializing for topology increases the upper bound on circuit depth by large constants; Shende et al. [2] mention a factor of 9, improved by Iten et al. [1] to $4\times$. The published approaches are hard to extend to different qubit gate sets, however, and it remains to be seen whether they can handle qutrits.⁴

Several techniques use numerical optimization, much as we did. They describe the gates in their variational/continuous representation and use optimizers and search to find a gate decomposition and instantiation. The work closest to ours is that of Martinez et al. [3], who use numerical optimization and brute-force search to synthesize circuits for a processor using trapped ion qubits. Their main advantage is the existence of all-to-all Mølmer-Sørensen gates, which allow a topology-independent approach. The main difference between our work and theirs is that they use randomization and genetic algorithms to search the solution space, while we show a more regimented way. When Martinez et al. describe their results, they claim that Mølmer-Sørensen counts are directly comparable to CNOT counts. By this metric, we seem to generate circuits comparable to or shorter than theirs. It is not clear how their approach behaves when topology constraints are present. The direct comparison is further limited by the fact that they consider only randomly generated unitaries, rather than algorithms or well-understood gates such as Toffoli or Fredkin.

Another topology-independent numerical optimization technique is presented in [4]. The main contribution is to use a quantum annealer to do searches over sequences of increasing gate depth. The authors report results only for two-qubit circuits.

All existing studies focus on the quality of the solution, rather than synthesis speed. They also report results for low-qubit concurrency: Khatri et al. [4] for two-qubit systems, Martinez et al. [3] for systems up to four qubits.

Solution Distinguishability: Synthesis algorithms can be classified as exact or approximate based on distinguishability. This is a subtle classification criterion, since many algorithms can be viewed as either. For example, the divide-and-conquer algorithm Meet-in-the-Middle proposed in [35], although designed for exact circuit synthesis, may also be used to construct an ϵ -approximate circuit. The results seem to indicate that the algorithm failed to synthesize a three-qubit QFT circuit. We classify our implementation as approximate since we rely on numerical optimization and therefore must accept solutions at a small distance from the original unitary.

11 Conclusion

In this paper we describe the LEAP compiler and modifications to a search and numerical-optimization-based synthesis algorithm. The results indicate that we can empirically provide optimal-depth circuits in a topology-aware manner for programs up to six qubits. The techniques employed prefix formation, incremental reoptimization, dimensionality reduction, and multistart optimization and can be easily generalized to other algorithms from this class. We believe LEAP provides the best-quality optimizer currently available for circuits up to six qubits.

LEAP has been released as part of the BQSket (Berkeley Quantum Synthesis Toolkit) infrastructure, and it is currently submitted for integration into IBM Qiskit.

⁴ [48] describes a method using Givens rotations and Householder decomposition.

Acknowledgments

This work was supported by the Advanced Quantum Testbed program and the Quantum Algorithm Teams program of the Advanced Scientific Computing Research for Basic Energy Sciences program, Office of Science of the U.S. Department of Energy under Contract No. DE-AC02-05CH11231 and DE-AC02-06CH11357.

References

- [1] Raban Iten, Roger Colbeck, Ivan Kukuljan, Jonathan Home, and Matthias Christandl. Quantum circuits for isometries. *Physical Review A*, 93:032318, Mar 2016. doi: 10.1103/PhysRevA.93.032318.
- [2] V. V. Shende, S. S. Bullock, and I. L. Markov. Synthesis of quantum-logic circuits. *IEEE Transactions on Computer-Aided Design of Integrated Circuits and Systems*, 25(6):1000–1010, June 2006. ISSN 0278-0070. doi: 10.1109/TCAD.2005.855930.
- [3] E. Martinez, T. Monz, D. Nigg, P. Schindler, and R. Blatt. Compiling quantum algorithms for architectures with multi-qubit gates. *ArXiv e-prints*, July 2016. doi: 10.1088/1367-2630/18/6/063029.
- [4] Sumeet Khatri, Ryan LaRose, Alexander Poremba, Lukasz Cincio, Andrew T. Sornborger, and Patrick J. Coles. Quantum-assisted quantum compiling. *arXiv e-prints*, art. arXiv:1807.00800, Jul 2018.
- [5] Robert R. Tucci. An Introduction to Cartan’s KAK Decomposition for QC Programmers. *arXiv e-prints*, art. quant-ph/0507171, Jul 2005.
- [6] M. G. Davis, E. Smith, A. Tudor, K. Sen, I. Siddiqi, and C. Iancu. Towards optimal topology aware quantum circuit synthesis. In *2020 IEEE International Conference on Quantum Computing and Engineering (QCE)*, pages 223–234, 2020. doi: 10.1109/QCE49297.2020.00036.
- [7] Ed Younis, Koushik Sen, Katherine Yelick, and Costin Iancu. QFAST: Quantum synthesis using a hierarchical continuous circuit space, 2020.
- [8] IBM Qiskit. Available at <https://qiskit.org/>.
- [9] Raban Iten, Oliver Reardon-Smith, Luca Mondada, Ethan Redmond, Ravjot Singh Kohli, and Roger Colbeck. Introduction to UniversalQCompiler. *arXiv e-prints*, art. arXiv:1904.01072, Apr 2019.
- [10] Victor Namias. The fractional order Fourier transform and its application to quantum mechanics. *IMA Journal of Applied Mathematics*, 25(3):241–265, 03 1980. ISSN 0272-4960. doi: 10.1093/imamat/25.3.241. URL <https://doi.org/10.1093/imamat/25.3.241>.
- [11] P. E. Hart, N. J. Nilsson, and B. Raphael. A formal basis for the heuristic determination of minimum cost paths. *IEEE Transactions on Systems Science and Cybernetics*, 4(2):100–107, July 1968. ISSN 0536-1567. doi: 10.1109/TSSC.1968.300136.
- [12] Jeffrey Larson and Stefan M. Wild. Asynchronously parallel optimization solver for finding multiple minima. *Mathematical Programming Computation*, 10(3), 2 2018. ISSN 1867-2949. doi: 10.1007/s12532-017-0131-4.
- [13] Sergey Bravyi, David Gosset, and Robert König. Quantum advantage with shallow circuits. *Science*, 362(6412):308–311, 2018. ISSN 0036-8075. doi: 10.1126/science.aar3106. URL <https://science.sciencemag.org/content/362/6412/308>.
- [14] Jarrod R McClean, Jonathan Romero, Ryan Babbush, and Alán Aspuru-Guzik. The theory of variational hybrid quantum-classical algorithms. *New Journal of Physics*, 18(2):23023, 2016. URL <http://iopscience.iop.org/article/10.1088/1367-2630/18/2/023023/>.

- [15] Dongbin Shin, Hannes Hübener, Umberto De Giovannini, Hosub Jin, Angel Rubio, and Noejung Park. Phonon-driven spin-Floquet magneto-valleytronics in MoS₂. *Nature Communications*, 9(1):638, 2018.
- [16] Lindsay Bassman, Kuang Liu, Aravind Krishnamoorthy, Thomas Linker, Yifan Geng, Daniel Shebib, Shogo Fukushima, Fuyuki Shimojo, Rajiv K Kalia, Aiichiro Nakano, et al. Towards simulation of the dynamics of materials on quantum computers. *Physical Review B*, 101(18):184305, 2020.
- [17] Mario Motta, Chong Sun, Adrian T. K. Tan, Matthew J. O’Rourke, Erika Ye, Austin J. Minnich, Fernando G. S. L. Brandão, and Garnet Kin-Lic Chan. Determining eigenstates and thermal states on a quantum computer using quantum imaginary time evolution. *Nature Physics*, 16(2):205–210, 2020. doi: 10.1038/s41567-019-0704-4. URL <https://doi.org/10.1038/s41567-019-0704-4>.
- [18] D Deutsch. Quantum computational networks. 425:73–90, 09 1989.
- [19] Vadym Kliuchnikov, Alex Bocharov, and Krysta M. Svore. Asymptotically optimal topological quantum compiling. *Physical Review Letters*, 112:140504, Apr 2014. doi: 10.1103/PhysRevLett.112.140504.
- [20] Nikolaus Hansen. The CMA evolution strategy: A tutorial. *CoRR*, abs/1604.00772, 2016. URL <http://arxiv.org/abs/1604.00772>.
- [21] Dong C. Liu and Jorge Nocedal. On the limited memory BFGS method for large scale optimization. *Mathematical Programming*, 45(1-3):503–528, 1989. doi: 10.1007/bf01589116.
- [22] Sameer Agarwal, Keir Mierle, and Others. Ceres solver. <http://ceres-solver.org>.
- [23] Laurens Van Der Maaten, Eric Postma, and Jaap Van den Herik. Dimensionality reduction: a comparative review. *J Mach Learn Res*, 10:66–71, 2009.
- [24] Vladislav Sovrasov. Comparison of dimensionality reduction schemes for derivative-free global optimization algorithms. *Procedia Computer Science*, 136:136–143, 2018. ISSN 1877-0509. doi: <https://doi.org/10.1016/j.procs.2018.08.246>. URL <https://www.sciencedirect.com/science/article/pii/S1877050918315515>. 7th International Young Scientists Conference on Computational Science, YSC2018, 02-06 July2018, Heraklion, Greece.
- [25] Stephen Hudson, Jeffrey Larson, Stefan M. Wild, David Bindel, and John-Luke Navarro. libEnsemble users manual. Technical Report Revision 0.7.2, Argonne National Laboratory, 2021. URL <https://buildmedia.readthedocs.org/media/pdf/libensemble/latest/libensemble.pdf>.
- [26] Stephen Hudson, Jeffrey Larson, John-Luke Navarro, and Stefan Wild. libEnsemble: A library to coordinate the concurrent evaluation of dynamic ensembles of calculations. *IEEE Transactions on Parallel and Distributed Systems*, 2021. doi: 10.1109/tpds.2021.3082815.
- [27] Ed Younis, Koushik Sen, Katherine Yelick, and Costin Iancu. QFAST: Conflating search and numerical optimization for scalable quantum circuit synthesis, 2021.
- [28] Xin-Chuan Wu, Marc Grau Davis, Frederic T. Chong, and Costin Iancu. Optimizing noisy-intermediate scale quantum circuits: A block-based synthesis, 2020.
- [29] Lindsay Bassman, Roel Van Beeumen, Ed Younis, Ethan Smith, Costin Iancu, and Wibe A. de Jong. Constant-depth circuits for dynamic simulations of materials on quantum computers, 2021.
- [30] C. M. Dawson and M. A. Nielsen. The Solovay-Kitaev algorithm. *Quant. Info. Comput.*, 6(1):81–95, 2005.
- [31] A. B. Nagy. On an implementation of the Solovay-Kitaev algorithm. *arXiv:quant-ph/0606077*, 2016.
- [32] O. Al-Ta’ani. *Quantum Circuit Synthesis using Solovay-Kitaev Algorithm and Optimization Techniques*. PhD thesis, Kansas State University, 2015.

- [33] A. De Vos and S. De Baerdemacker. Block- ZXZ synthesis of an arbitrary quantum circuit. *Phys. Rev. A*, 94:052317, Nov 2016. doi: 10.1103/PhysRevA.94.052317. URL <https://link.aps.org/doi/10.1103/PhysRevA.94.052317>.
- [34] Alex Bocharov and Krysta M. Svore. Resource-optimal single-qubit quantum circuits. *Phys. Rev. Lett.*, 109:190501, Nov 2012. doi: 10.1103/PhysRevLett.109.190501. URL <https://link.aps.org/doi/10.1103/PhysRevLett.109.190501>.
- [35] Matthew Amy, Dmitri Maslov, Michele Mosca, and Martin Roetteler. A meet-in-the-middle algorithm for fast synthesis of depth-optimal quantum circuits. *Trans. Comp.-Aided Des. Integ. Cir. Sys.*, 32(6):818–830, June 2013. ISSN 0278-0070. doi: 10.1109/TCAD.2013.2244643. URL <http://dx.doi.org/10.1109/TCAD.2013.2244643>.
- [36] Esteban A Martinez, Thomas Monz, Daniel Nigg, Philipp Schindler, and Rainer Blatt. Compiling quantum algorithms for architectures with multi-qubit gates. *New Journal of Physics*, 18(6):063029, 2016. URL <http://stacks.iop.org/1367-2630/18/i=6/a=063029>.
- [37] B. Giles and P. Selinger. Exact synthesis of multiqubit Clifford+T circuits. *Physical Review Letters.*, 87(3):032332, March 2013. doi: 10.1103/PhysRevA.87.032332.
- [38] S. S. Bullock and I. L. Markov. An arbitrary two-qubit computation in 23 elementary gates or less. In *Proceedings 2003. Design Automation Conference (IEEE Cat. No.03CH37451)*, pages 324–329, June 2003. doi: 10.1109/DAC.2003.1219017.
- [39] J. Urias. Householder factorization of unitary matrices. *J. Mathematical Physics*, 51:072204, 2010.
- [40] Mikko Möttönen, Juha J. Vartiainen, Ville Bergholm, and Martti M. Salomaa. Quantum circuits for general multiqubit gates. *Phys. Rev. Lett.*, 93:130502, Sep 2004. doi: 10.1103/PhysRevLett.93.130502. URL <https://link.aps.org/doi/10.1103/PhysRevLett.93.130502>.
- [41] M. Amy and M. Mosca. T-count optimization and Reed-Muller codes. *arXiv:1601.07363v1*, 2016.
- [42] G. Seroussi and A. Lempel. Factorization of symmetric matrices and trace-orthogonal bases in finite fields. *SIAM Journal on Computing*, 9(4):758–767, 1980. doi: 10.1137/0209059. URL <https://doi.org/10.1137/0209059>.
- [43] Neil J. Ross. Optimal ancilla-free Clifford+V approximation of Z-rotations. *Quantum Info. Comput.*, 15(11-12):932–950, September 2015. ISSN 1533-7146. URL <http://dl.acm.org/citation.cfm?id=2871350.2871354>.
- [44] V. Kliuchnikov, D. Maslov, and M. Mosca. Practical approximation of single-qubit unitaries by single-qubit quantum Clifford and T circuits. *IEEE Transactions on Computers*, 65(1):161–172, Jan 2016. ISSN 0018-9340. doi: 10.1109/TC.2015.2409842.
- [45] *Classical and Quantum Computation*. American Mathematical Society, Boston, MA, 2012.
- [46] Adam Paetznick and Krysta M. Svore. Repeat-until-success: Non-deterministic decomposition of single-qubit unitaries. *Quantum Info. Comput.*, 14(15-16):1277–1301, November 2014. ISSN 1533-7146. URL <http://dl.acm.org/citation.cfm?id=2685179.2685181>.
- [47] Robert R. Tucci. A rudimentary quantum compiler. *arXiv e-prints*, art. quant-ph/9902062, Feb 1999.
- [48] Nikolay Vitanov. Synthesis of arbitrary $SU(3)$ transformations of atomic qutrits. *Phys. Rev. A*, 85, 03 2012. doi: 10.1103/PhysRevA.85.032331.

The submitted manuscript has been created by UChicago Argonne, LLC, Operator of Argonne National Laboratory (“Argonne”). Argonne, a U.S. Department of Energy Office of Science laboratory, is operated under Contract No. DE-AC02-06CH11357. The U.S. Government retains for itself, and others acting on its behalf, a paid-up nonexclusive, irrevocable worldwide license in said article to reproduce, prepare derivative works, distribute copies to the public, and perform publicly and display publicly, by or on behalf of the Government. The Department of Energy will provide public access to these results of federally sponsored research in accordance with the DOE Public Access Plan <http://energy.gov/downloads/doe-public-access-plan>.